LJMU Research Online

Zhang, C-Y, Pan, R-R, Zhang, X-D, Zhou, Y, Ye, Y, Xia, J, Rahman, K, Zhang, H and Zhu, J-Y

 New tetracyclic triterpenoids from Jatropha gossypiifolia induce cell-cycle arrest and apoptosis in RKO cells.

http://researchonline.ljmu.ac.uk/id/eprint/9333/

Article

For more information please contact researchonline@ljmu.ac.uk

Antitumor Activity of Diterpenoids from *Jatropha gossypiifolia*: Cell Cycle Arrest and Apoptosis-Inducing Activity in RKO Colon Cancer Cells

Chun-Yan Zhang,[†] Li-Jun Zhang,[†] Zhi-Cheng Lu,[‡] Chen-Yun Ma,[‡] Ying Ye,[†] Khalid Rahman,[§] Hong Zhang,*,[†] and Jian-Yong Zhu*,[†]

[†]Central Laboratory, Seventh People's Hospital of Shanghai University of TCM, Shanghai 200137, People's Republic of China

[‡]Medical Laboratory, Seventh People's Hospital of Shanghai University of TCM, Shanghai 200137, People's Republic of China

[§]Faculty of Science, School of Pharmacy and Biomolecular Sciences, Liverpool John Moores University, Liverpool L3 3AF, U.K.

ABSTRACT: Nine new minor diterpenoids, jatrogossones A−I (**1−9**), and six known analogues (**10−15**) were separated from an extract of the branches and leaves of *Jatropha gosspiifolia*. Compounds **4−6** and **10**, possessing a 5/11 fused-ring skeleton, and **8**, **9**, and **13** with a 5/9/5 fused-ring skeleton represent rare diterpenoid skeletons that have been found only in compounds isolated from plants of the *Jatropha* genus. The absolute configurations of **1−10** were defined by using a combination of electronic circular dichroism data analysis and single-crystal X-ray diffraction data. The cytotoxicity of the diterpenoids were evaluated using RKO and LOVO colon cancer cells in which regenerating islet-derived protein 3-alpha (Reg3A) is highly expressed. Compound **12** exhibited cytotoxicity against RKO colon cancer cells with an IC_{50} value of 2.6 μM. Morphological features of apoptosis and antimigration activities were evaluated in **12**-treated RKO cells. Compound **12** effectively induced apoptosis of RKO, which was associated with G_2/M-phase cell cycle arrest. Flow cytometric analysis showed that the treatment by **12** significantly induced RKO cell apoptosis in a dose-dependent manner.

Colorectal cancer (CRC) is the third and the second most commonly diagnosed tumor in men and women, respectively, worldwide.[1] In the U.S. alone, approximately 140 000 people are diagnosed annually with CRC, and among these, 50 000 have died of this malignant disease.[2] Considering the high morbidity and low effectiveness of colon cancer treatment, there is a need for new strategies that can prevent and cure this disease. Colorectal carcinogenesis is a multistep process that offers opportunities for preventive interventions.[3] The critical role of Reg3A has been well-established in CRC, and selective Reg3A inhibitors have recently been regarded as an elegant example for CRC chemoprevention.[4] Therefore, identifying new preventive agents against Reg3A is thought to be an essential step towards the discovery of molecular targets for CRC chemoprevention.

Jatropha gossypiifolia L. (Euphorbiaceae) is widely distributed in countries of tropical, subtropical, and dry tropical weather and tropical semiarid regions of Africa and the Americas.[5] It is used in folk medicine for various purposes, such as analgesic, anti-inflammatory, antihemorrhagic, hemostatic, and an antidote for snakebites.[5,6] Previous phytochemical investigations of *J. gossypiifolia* led to the isolation of numerous diterpenoids,[7-10] lignans,[11,12] cyclic peptides,[13] and triterpenoids,[14] some of which showed anticancer[9] and antibacterial activities.[7] As part of an ongoing effort to discover natural products with anticancer activities,[15,16] the petroleum ether fraction of *J. gossypiifolia* showed inhibitory activities against a panel of human cancer cells. Chemical investigation of petroleum ether extracts led to the isolation of nine new diterpenoids (**1−9**) and six known analogues (**10−15**).

Compounds **1**−**15** displayed cytotoxicity against RKO and LOVO colon cancer cells, with IC_{50} values in the range of 2.6 to 18.6 μM. Herein, the isolation, structural elucidation, and assessment of compound **12**'s ability to induce apoptosis and arrest the cell cycle in RKO human colon cancer cells are reported.

RESULTS AND DISCUSSION

Compound **1** had a molecular formula of $C_{22}H_{30}O_4$, as established by the HRESIMS ion at m/z 376.2479 $[M + NH_4]^+$ (calcd for $C_{22}H_{34}O_4N$, 376.2482). The IR absorption bands at 1735, 1717, and 1686 cm^{-1} were indicative of the presence of ester carbonyl and conjugated carbonyl functionalities. Its ^1H NMR data indicate the presence of six methyl groups [δ_H 2.01 (3H, s), 1.77 (3H, d, $J = 1.3$ Hz), 1.19 (3H, s), 1.16 (3H, d, $J = 7.1$ Hz), 1.13 (3H, s), and 1.00 (3H, d, $J = 6.4$ Hz)] and two double bonds [δ_H 5.86 (1H, dd, $J = 10.4, 2.1$ Hz) and 5.78 (1H, dd, $J = 9.7, 1.3$ Hz)]. The ^{13}C NMR spectrum of **1** resolved 22 carbon resonances comprising two double bonds (δ_C 142.0, 134.3, 139.9, and 131.3), an ester carbonyl group (δ_C 170.3 and 21.2), two ketocarbonyl groups (δ_C 213.6 and 204.0), a quaternary carbon, five methyls, six methines (one oxygenated), and two methylenes. As five of the eight indices of hydrogen deficiency were accounted for by an ester carbonyl, two double bonds, and two ketocarbonyls, the remaining three indices of hydrogen deficiency required that **1** was tricyclic. The aforementioned spectroscopic data are similar to those of jatrointelones A−G isolated from the other species in the same genus,[16] implying that **1** likely possessed the same carbon frameworks. Three subunits, **a** (C-1 to C-3; C-16), **b** (C-5 to C-6; C-17), and **c** (C-8 to

C-9; C-11 to C-12) [Figure S1, Supporting Information], were established via the ^{1}H-^{1}H COSY data. The linkage of subunits **a**−**c** and other functionalities were deduced by the HMBC correlations (Figure S1, Supporting Information). The HMBC cross-peaks from H-5 to C-4, C-6, and C-15 and H-12 to C-13, C-14, and C-20, established the $\Delta^{4(5)}$ and $\Delta^{12(13)}$ double bonds, while the correlations from H$_3$-18 to C-11, C-10, and C-9 established the cyclopropane ring. The HMBC correlation from H-3 (δ_H 5.41, d, $J = 4.9$ Hz) to the acetoxy carbonyl at δ_C 170.3 revealed that the acetoxy group was located at C-3. The HMBC correlations from H$_3$-17 (δ_H 1.16, d, $J = 7.1$ Hz) and H-9 (δ_H 1.62) to C-7 suggested that a C-7 carbonyl group (δ_C 213.6). The relative configuration of **1** was elucidated by the NOESY experiment (Figure S1, Supporting Information). The key NOESY interactions of H-15/H-6 and H-11/CH$_3$-20, assigned the $\Delta^{4(5)}$ and $\Delta^{12(13)}$ double bonds as *E* configured. In the NOESY spectra, the correlations of H-9/H-11 suggested a *cis*-orientation for the *β*-oriented dimethylcyclopropane moiety. Thus, the NOESY cross-peaks of H-8*β*/CH$_3$-19, CH$_3$-19/H-12, H-12/H-15, H-15/H-6, H-1*β*/H-3, and H-3/H-5 assigned H-15, H-3, and H-6 as *β*, while H$_3$-16 was assigned an *α*-orientation according to the correlations of H$_3$-16/H-1*α* (Figure S1, Supporting Information). The structure of **1** was confirmed through Cu K*α* X-ray diffraction data analysis [Flack parameter, −0.2 (2)] (Figure 1). The absolute configuration of **1** was confirmed by experimental and calculated ECD data as 2*R*,3*R*,6*R*,9*S*,11*R*,15*S*-**1** (Figure S2, Supporting Information). Thus, the structure of jatrogossone A (**1**) was established as (+)-(4*E*,12*E*,2*R*,3*R*,6*R*,9*S*,11*R*,15*S*)-3-acetoxylathyr-4,12-dien-7,14-dione.

Compound **2** exhibited a molecular formula of C$_{22}$H$_{30}$O$_5$, an oxygen atom mass unit

more than that of jatrogossone A (**1**). The NMR spectra of **2** showed a close structural resemblance to those of **1**, except for the presence of a hydroxy group in **2**, indicating that it was the oxygenated derivative of **1**. The C-15 location of the hydroxy group was deduced by comparison of the ^{13}C NMR chemical shift value of C-15 (δ_C 51.7 in **1**) and (δ_C 83.3 in **2**). The relative configuration of **2** was determined via the NOESY and NMR data, which showed the same features as those of **1**. Compound **1** was assigned the same absolute configuration as **2** based on their similar ECD spectra, which included Cotton effects at 309 nm ($\Delta\varepsilon$ +2.95), 265 nm ($\Delta\varepsilon$ −3.54), and 220 nm ($\Delta\varepsilon$ −8.84), due to the n → π^* (above 300 nm) and π → π^* (230−300 nm) transitions of the α,β-unsaturated carbonyl moiety (Figure S3, Supporting Information). Thus, the structure of jatrogossone B (**2**) was identified as (−)-(4*E*,12*E*,2*R*,3*R*,6*R*,9*S*,11*R*,15*R*)-3-acetoxylathyr-4,12-dien-15-ol-7,14-dione.

Compound **3** was assigned a molecular formula, $C_{22}H_{32}O_4$ by its HRESIMS and ^{13}C NMR data. The 1D NMR data of **3** showed close similarities those of **1**, with the major differences being that a trisubstituted double bond in **3** was replaced by an sp^3 methine C-13 (δ_C 43.9) and an sp^3 methylene C-12 (δ_C 28.4) in **1**, indicating that **3** is a 12,13-dihydrogenated derivative of **1**. This inference was confirmed by key HMBC correlations from H$_3$-20 (δ_H 1.11) to C-13 and C-12, as well as the ^1H–^1H COSY correlations between H-12, H-13, and H-20. The NOESY correlations of H-13/H-15, H-15/H-2, H-15/H-3, H-15/H-6, H-6/H-13, H-6/H-8β, and H-8β/CH$_3$-19 assigned H-15, H-13, H-2, H-3, and H-6 as β-oriented, while CH$_3$-20 was assigned an α-orientation. Thus, the relative configuration of **3** was determined to be

$2R^*,3R^*,6R^*,9S^*,11R^*,13R^*,15S^*$. The absolute configuration of **3** was elucidated by comparing its calculated and experimental ECD spectra. The calculated ECD spectrum for enantiomer $2R,3R,6R,9S,11R,13R,15S$ showed a good fit with the experimental curve of **3** (Figure 2). Accordingly, the structure of jatrogossone C (**3**) was defined as (+)-($4E,2R,3R,6R,9S,11R,13R,15S$)-3-acetoxylathyr-4-en-7,14-dione.

Compound **4** had a molecular formula of $C_{22}H_{30}O_5$, which was deduced from the HRESIMS spectrum (m/z 419.2073, $[M + HCOO]^-$). The ^1H NMR data of **4** revealed resonances characteristic for three olefinic protons [δ_H 6.06 (1H, d, J = 1.8 Hz), 5.60 (1H, dd, J = 15.4, 9.7 Hz), and 5.23 (1H, dd, J = 15.4, 9.2 Hz)], an oxygenated sp^3 methine proton [δ_H 5.27 (1H, d, J = 4.6 Hz)], two terminal alkene methylene protons (H$_2$-19) at δ_H 4.81 and 4.79, and five methyl groups [δ_H 2.10 (3H, s), 1.75 (3H, s), 1.37 (3H, s), 1.24 (3H, d, J = 6.9 Hz), and 1.02 (3H, d, J = 6.8 Hz)]. Analysis of the ^{13}C NMR data using DEPT revealed 22 carbon resonances comprising two ketocarbonyl groups (δ_C 212.4 and 208.6), three double bonds (δ_C 146.2, 140.2, 134.8, 134.4, 131.5, and 110.4), an ester carbonyl group (δ_C 170.9 and 21.3), an oxygenated tertiary carbon (δ_C 80.3), two methylenes, four methyls, and five sp^3 methines (one oxygenated). The aforementioned information resembles those of the co-occurring known diterpenoid, integerrimene (**10**) [17], except for the presence of an oxygenated tertiary carbon in **4**, indicating that it was the oxygenated derivative of **10**. The hydroxylation at C-6 was verified by the HMBC correlations from both H$_3$-17 (δ_H 1.37) and H-5 (δ_H 6.06) to C-6. The key NOESY interaction of H-15/OH-6 and a coupling constant of 15.4 Hz between H-11 and H-12, assigned the $\Delta^{4(5)}$ and $\Delta^{11(12)}$ double bonds as E configured.

The NOESY correlations of H-8β/H-11, H-11/H-13, H-13/H-15, H-15/OH-6, H-15/H-3 assigned H-3, HO-6, H-13, and H-15 as β-oriented, while correlations of H$_3$-16/H-1α and H-9/H-8α assigned H$_3$-16 and H-9 as α-orientated (Figure S4, Supporting Information). Compound 4 was assigned the same absolute configuration as 10 based on their similar ECD spectra, which included Cotton effects at 200 nm ($\Delta\varepsilon$ +8.66) and 310 nm ($\Delta\varepsilon$ −2.23) (Figure S5, Supporting Information). The structure of compound 10 including absolute configuration was confirmed through Cu Kα X-ray diffraction data analysis [Flack parameter, 0.15 (11)] (Figure 3). Therefore, the structure of jatrogossone D (4) was established as (−)-(4E,12E,2R,3R,6S,9S,13R,15S)-3-acetoxy-10,11-secolathyr-4,11-dien-6-ol-7,14-dione.

Compound 5 was assigned a molecular formula of C$_{20}$H$_{28}$O$_3$ from the HRESIMS data (m/z 334.2376 [M + NH$_4$]$^+$). The NMR data of 5 resembled those of 10, except for the absence of signals for an acetyl group and supported by an upfield-shifted resonance of H-3 at δ_H 4.00 (1H, dd, J = 10.2, 4.0 Hz), indicating that 5 was the 3-deacetylated derivative of 10. The relative configuration of 5 was determined via the NOESY and NMR data, which showed the same features as those of 10. Compound 5 was assigned the same absolute configuration as 10 based on their similar ECD spectra (Figure S5, Supporting Information). Thus, the structure of jatrogossone E (5) was determined as (−)-(4E,12E,2R,3R,6R,9S,13R,15S)-10,11-secolathyr-4,11-dien-3-ol-7,14-dione.

Compound 6 had a molecular formula of C$_{22}$H$_{30}$O$_4$, as established by the HRESIMS ion at m/z 381.2029 [M + Na]$^+$ (calcd for C$_{22}$H$_{30}$O$_4$Na, 381.2036). The NMR spectra of 6 closely resembled those of 10, except for replacement of the $\Delta^{4(5)}$ double bond in 10

by the $\Delta^{5(6)}$ double bond in **6**. The location of the $\Delta^{5(6)}$ double bond was supported by HMBC cross-peaks from H₃-17 (δ_H 1.93) to C-5, C-6, and C-7. The NOESY correlations of H-15/H-4 and H-4/H-2 assigned a β-orientation for H-4. Compound **6** was assigned the same absolute configuration as **10** based on their similar ECD spectra, which included Cotton effects at 200 nm ($\Delta\varepsilon$ +5.62) and 297 nm ($\Delta\varepsilon$ −2.20) (Figure S5, Supporting Information). Hence, the structure of jatrogossone F (**6**) was defined as (−)-(5*Z*,11*E*,2*R*,3*R*,4*S*, 9*S*,13*R*,15*S*)-3-acetoxy-10,11-secolathyr-5,11-dien-7,14-dione.

Compound **7**, an amorphous solid, had a molecular formula of $C_{22}H_{32}O_4$ as established by the HRESIMS ion at *m/z* 378.2644 $[M + NH_4]^+$, corresponding to seven indices of hydrogen deficiency. Its ¹H NMR data indicate the presence of an olefinic proton [δ_H 5.80 (1H, dd, *J* = 3.3, 3.2 Hz)], an oxygenated sp³ methine proton [δ_H 5.40 (1H, d, *J* = 3.6 Hz)], and six methyl groups [δ_H 0.94 (3H, s), 0.97 (3H, d, *J* = 6.2 Hz), 1.06 (3H, s), 1.13 (3H, d, *J* = 7.3 Hz), 1.23 (3H, d, *J* = 6.9 Hz), and 2.01 (3H, s)]. The ¹³C NMR spectrum of **7** revealed 22 carbon resonances including a ketocarbonyl group (δ_C 207.3), a trisubstituted double bond (δ_C 144.9 and 132.1), an ester carbonyl group (δ_C 170.6 and 21.4), five methyls, eight sp³ methines (one oxygenated), two methylenes, a quaternary carbon, and an oxygenated tertiary carbon. The abovementioned analysis accounted for three out of seven indices of hydrogen deficiency, suggesting that **7** had a tetracyclic carbon backbone. These data were similar to those of **3**, except for the difference of ring topology, indicating the linkage between C-8 and C-14 in **7**. This tetracyclic ring topology was also supported by the putative biosynthetic pathway.[18] Finally, this deduction was verified by HMBC cross-peaks from H₃-20 (δ_H 1.13) to C-

14 and H-8 (δ_H 2.22) to C-7, C-9, C-13, C-14, and C-15. The detailed interpretation (Figure S6, Supporting Information) of its 2D NMR data allowed the establishment of the 2D structure of **7**. The relative configuration of 7 was assigned as similar to **3** by analyzing the NOESY data (Figure S6, Supporting Information). The NOESY cross-peaks of CH$_3$-19/H-12β, CH$_3$-19/H-8, and H-8/H-15 assigned H-8 as β-oriented, while HO-14 was assigned an α-orientation according to the correlations of HO-14/H-1α, and HO-14/H$_3$C-20. Thus, the relative configuration of **7** was assigned as 2R^*,3R^*,6R^*,8S^*,9R^*,11R^*,13R^*,14S^*,15S^*. The absolute configuration of **7** was confirmed by comparing its calculated and experimental ECD spectra. The calculated ECD spectrum for enantiomer 2R,3R,6R,8S,9R,11R,13R,14S,15S showed a good fit with the experimental curve of **7** (Figure 4). Therefore, the structure of jatrogossone G (**7**) was defined as (+)-(4E,2R,3R,6R,8S,9R,11R,13R,14S,15S)-3-acetoxytiglia-4-en-14-ol-7-one.

Compound **8** was obtained as colorless crystals. The HRESIMS data exhibited a sodium adduct ion [M + Na]$^+$ at m/z 337.1799 (calcd for 337.1774 corresponding to a molecular formula of C$_{20}$H$_{26}$O$_3$. The ^{1}H NMR data exhibited resonances characteristic of an olefinic proton [δ_H 5.82 (1H, s)] and five methyl groups [δ_H 1.91 (3H, d, J = 1.6 Hz), 1.36 (3H, s), 1.28 (3H, s), 1.07 (3H, d, J = 6.9 Hz), and 0.88 (3H, s)]. The ^{13}C NMR spectrum exhibited the presence of 20 carbon resonances, including three ketocarbonyl groups (δ_C 215.3, 213.3, and 208.0), two double bonds (δ_C 141.9, 138.3, 141.6, and 127.6), five methyls, four methylenes, two methines, and two quaternary carbons. As five of the eight indices of hydrogen deficiency were accounted for by two

double bonds and three ketocarbonyl groups, the remaining three indices of hydrogen deficiency required that **8** was tricyclic. These spectroscopic data are similar to those of jatrophatrione,[19] which was isolated from other species in the same genus. Comparison with jatrophatrione, showed that a $\Delta^{3(4)}$ double bond in jatrophatrione was replaced by a $\Delta^{4(15)}$ double bond in **8**. This assignment was verified by HMBC correlations from H-3a (δ_H 2.59) to C-15 (δ_C 138.3). The relative configuration of **8** was the same as that of jatrophatrione by analysis of the NOESY correlations (Figure S7, Supporting Information). The absolute configuration of **8** was confirmed through Cu Kα X-ray diffraction data analysis [Flack parameter, 0.12 (13] (Figure 5). Consequently, the structure of compound **8** was elucidated and named jatrogossone H.

Compound **9** had the same molecular formula ($C_{20}H_{26}O_3$) as **8** based on their HRESIMS data. The NMR data of **9** closely resembled those of **8**, with differences being due to the orientation of CH$_3$-16 (δ_H 1.03 and δ_C 20.9 in **9**; δ_H 1.07 and δ_C 21.7 in **8**), indicating that compound **9** was a C-2 epimer of **8**. Therefore, the β-oriented CH$_3$-16 group was assigned in **9**. Compound **9** was assigned the same absolute configuration as **8** based on their similar ECD spectra, which included Cotton effects at 250 nm ($\Delta\varepsilon$ +1.07) and 323 nm ($\Delta\varepsilon$ +0.51) (Figure S8, Supporting Information). Therefore, the structure of jatrogossone I (**9**) was assigned as shown.

Additionally, six known compounds were identified as integerrimene (**10**),[17] jatrophone (**11**),[10] jatrogrossidione (**12**),[20] citlalitrione (**13**),[21] jatropholone B (**14**),[8] and jatropholone A (**15**).[8]

Cytotoxic Effect of Isolates Against RKO and LOVO Cells. The growth inhibitory

properties of the 5-fluorouracil (5-FU) and 15 diterpenoids (**1**−**15**) were investigated by the CCK-8 metabolism assay, and the IC_{50} values were calculated after 48 h of treatment. We considered any diterpenoid compound exhibiting an inhibition rate of less than 50% at 20 μM to be inactive. The results showed that compounds **1**−**10** and **13**−**15** did not inhibit RKO and LOVO growth, while compounds **11** and **12** showed moderate inhibitory activities with IC_{50} values on LOVO at 18.6 and 14.5 μM, respectively. Compounds **11** and **12** were the most active compounds with IC_{50} values on RKO at 8.0 and 2.6 μM, respectively; the positive 5-Fu positive control had IC_{50} values on RKO and LOVO of 10.2 and 11.5 μM (Figure 6), respectively.

Morphological Changes of RKO Cells Treated with Jatrogrossidione (12). To investigate the mechanism underlying the antitumor activity of compound **12**, RKO cells were further examined in fluorescence photomicrographs of RKO cells stained with DAPI after treatment for 24 h with 2.6 and 5.2 μM of **12**. Afterwards, the morphological characteristic features of apoptosis were examined under fluorescence or inverted light microscopy. The fragmentation of the nucleus, condensation of chromatin, and morphological characteristic features of apoptosis were examined. Control cells showed homogeneous and round nuclei, whereas cells treated with **12** showed condensed and fragmented nuclei (arrows) (Figure 7). As shown in Figure 7, a 2-fold increase in IC_{50} to 5.2 μM induces a significant increase of apoptosis in RKO cells.

Antimigratory Activity of Jatrogrossidione (12) in RKO Cells. The wound-healing properties were used as a tool to study the directional cell migration in vitro.[22]

The effects of **12** in inhibiting the migration of RKO cells were examined by wound-healing assays. To investigate the effect of **12** on migration, RKO cells were treated with 2.6 and 5.2 μM of **12** for 48 h. After incubation, the wound was measured by comparing it to the original wound width. This analysis method was used to assess the antimigration activity of diterpenoids. Compared with the positive control 5-FU, the comparable antimigration activity of **12** is shown on RKO cells in Figure 8.

Jatrogrossidione (12) Induces Cell Cycle Arrest at the G$_2$/M Phase in RKO Cells. To elucidate the mechanism of the anti-proliferative activity of **12**, its effect on cell cycle distribution was analyzed by flow cytometry. As shown in Figure 9, compound **12** arrested the growth of cells at the G$_2$/M phase, increasing from 10.97% of cells treated with the negative control to 18.30% and 25.76% of cells treated with 2.6 and 5.2 μM of **12**, respectively. These results show that **12** inhibits proliferation of RKO cells via the induction of G$_2$/M phase arrest.

Jatrogrossidione (12) Causes RKO Cell Death by Apoptosis. To clarify the mechanism of **12-**induced RKO cell death, annexin V-FITC and propidium iodide (PI) co-staining and flow cytometric analysis were performed. As shown in Figure 10, compound **12** could induce efficient apoptosis of RKO. When compared with the control (5.89%, early and late apoptosis), treatment with **12** increased the apoptosis rates, which gradually increased from 39.7 to 89.7% after treatment with 2.6 and 5.2 μM of **12**, respectively. The results show that **12** caused a remarkable increase in cellular apoptosis in a dose-dependent manner.

EXPERIMENTAL SECTION

13

General Experimental Procedures. The detailed instruments and spectroscopic measurements for the purified compounds and the materials for the isolation of the diterpenoids from *J. gossypiifolia* are presented in the .

Plant Material. Branches and leaves of *J. gossypiifolia* were collected in November 2015, Shennong Herbal Garden, Guangzhou city, People's Republic of China, and was identified by Professor L.-P. Qin. A sample (SJGZ-201511) was deposited at our Central Laboratory.

Extraction and Isolation. The branches and leaves of *J. gossypiifolia* (5 kg) were pulverized and soaked with 95% ethanol (3 × 25L) at room temperature, and the solvent was evaporated in vacuo to give a crude extract (121 g). The concentrated extract was suspended in H_2O and fractionated with petroleum ether and EtOAc, respectively. The petroleum ether extract (31 g) was chromatographed over MCI gel with MeOH/H_2O (30% to 100%, v/v) to afford four fractions (I−IV). Fr. II (6.0 g) was separated on a Sephadex LH-20 column with MeOH to give four fractions (IIa−IId). Fr. IIb (1.8 g) was passed through a silica gel (petroleum ether/EtOAc, 1:0 → 0:1, v/v) to give Fr. IIb1–Fr. IIb3. Fr. IIb2 was separated over a column of Sephadex LH-20 with MeOH/CH_2Cl_2 (1:1, v/v) to give **2** (10.2 mg). Fr. IIb3 was purified by a semi-preparative method with a YMC column (MeOH/H_2O, 7:3), to give **14** (6.1 mg) and **15** (7.2 mg). Fr. IIc (2.9 g) was chromatographed on a silica gel column using gradient elution with petroleum ether/EtOAc to yield three fractions (IIc1–IIc3). Fr. IIc2 was purified by reversed-phase HPLC (MeOH/H_2O,

7:3) to yield **7** (6.1 mg) and **12** (8.8 mg). Fr. IIc3 was separated by RP-HPLC (MeOH/H$_2$O, 7:3), to give **8** (4.2 mg), **9** (2.5 mg), and **13** (2.5 mg). Fr.III (6.5 g) was separated over a column of Sephadex LH-20 with MeOH to afford five fractions (IIIa−IIIe). Fr. IIIa (3.2 g) was separated over an RP-C$_{18}$ column with gradient elution with MeOH/H$_2$O to give four fractions (IIIa1−IIIa4). Fr. IIIa2 was separated over a column of Sephadex LH-20 with MeOH/CH$_2$Cl$_2$ (1:1) to yield **6** (7.2 mg). Fr. IIIa3 was separated over RP-HPLC (H$_2$O/MeOH, 2:8), to give **2** (6.8 mg), **1** (6.2 mg), and **3** (5.8 mg). Fr. IIIb (2.0 g) was separated over a column of Sephadex LH-20 to yield Fr. IIIb1−Fr. IIIb3. Fr. IIIb1 was separated by RP-HPLC (H$_2$O/MeOH, 4:6), to yield **5** (4.5 mg), **4** (5.4 mg), and **10** (11.2 mg).

Jatrogossone A (1): colorless crystals; mp 165−167 °C; $[\alpha]^{25}_D$ +45 (*c* 0.2, MeOH); UV (MeOH) λ_{max} (log ε) 207 (3.96), 262 (3.84) nm; ECD (*c* 1.2 × 10^{-4} M, MeOH) λ_{max} ($\Delta\varepsilon$) 223 (−7.28), 290 (+2.28) nm; IR (KBr) ν_{max} 2931, 1735, 1717, 1686, 1454, 1371, 1237, 1058, 868 cm^{-1}; ^{1}H and ^{13}C NMR, see Tables 1 and 2; HRESIMS *m/z* 376.2479 [M + NH$_4$]$^+$ (calcd for C$_{22}$H$_{34}$O$_4$N, 376.2482).

Jatrogossone B (2): an amorphous solid; $[\alpha]^{25}_D$ −24 (*c* 0.2, MeOH); UV (MeOH) λ_{max} (log ε) 208 (4.33), 267 (4.13) nm; ECD (*c* 1.3 × 10^{-4} M, MeOH) λ_{max} ($\Delta\varepsilon$) 220 (−8.84), 309 (+2.95) nm; IR (KBr) ν_{max} 3459, 2926, 2930, 1737, 1709, 1664, 1595, 1370, 1235, 1048, 898 cm^{-1}; ^{1}H and ^{13}C NMR, see Tables 1 and 2; HRESIMS *m/z* 397.1971 [M + Na]$^+$ (calcd for C$_{22}$H$_{30}$O$_5$Na, 397.1985).

Jatrogossone C (3): an amorphous solid; $[\alpha]^{25}_D$ +42 (*c* 0.1, MeOH); UV (MeOH) λ_{max} (log ε) 210 (3.78), 264 (2.84), 300 (3.95) nm; ECD (*c* 1.4 × 10^{-4} M, MeOH) λ_{max}

($\Delta\varepsilon$) 229 (−2.84), 296 (+4.10) nm; IR (KBr) ν_{max} 2961, 2931, 1732, 1706, 1455, 1371, 1237, 1049, 886 cm^{-1}; ^{1}H and ^{13}C NMR, see Tables 1 and 2; HRESIMS m/z 378.2638 [M + NH$_4$]$^+$ (calcd for C$_{22}$H$_{36}$O$_4$N, 378.2638).

Jatrogossone D (4): an amorphous solid; $[\alpha]^{25}_D$ −16 (*c* 0.2, MeOH); UV (MeOH) λ_{max} (log ε) 208 (3.61) nm; ECD (*c* 1.3 × 10^{-4} M, MeOH) λ_{max} ($\Delta\varepsilon$) 200 (+8.67), 310 (−2.23) nm; IR (KBr) ν_{max} 2928, 1714, 1456, 1377, 1239, 1020 cm^{-1}; ^{1}H and ^{13}C NMR, see Tables 1 and 2; HRESIMS m/z 419.2073 [M + COOH]$^-$ (calcd for C$_{23}$H$_{31}$O$_7$, 419.2075).

Jatrogossone E (5): an amorphous solid; $[\alpha]^{25}_D$ −11 (*c* 0.2, MeOH); UV (MeOH) λ_{max} (log ε) 208 (3.41) nm; ECD (*c* 1.5 × 10^{-4} M, MeOH) λ_{max} ($\Delta\varepsilon$) 200 (+5.03), 300 (−1.84) nm; IR (KBr) ν_{max} 2925, 1734, 1710, 1456, 1376, 1236, 1019, 976, 891 cm^{-1}; ^{1}H NMR see Table 1 and ^{13}C NMR see Table 2; HRESIMS m/z 334.2376 [M + NH$_4$]$^+$ (calcd for C$_{20}$H$_{32}$O$_3$N, 334.2377).

Jatrogossone F (6): an amorphous solid; $[\alpha]^{25}_D$ −184 (*c* 0.1, MeOH); UV (MeOH) λ_{max} (log ε) 209 (3.87) nm; ECD (*c* 1.1 × 10^{-4} M, MeOH) λ_{max} ($\Delta\varepsilon$) 200 (+5.62), 297 (−2.20) nm; IR (KBr) ν_{max} 2929, 1735, 1710, 1456, 1375, 1238, 1018, 975 cm^{-1}; ^{1}H NMR see Table 1 and ^{13}C NMR see Table 2; HRESIMS m/z 381.2029 [M + Na]$^+$ (calcd for C$_{22}$H$_{30}$O$_4$Na, 381.2036).

Jatrogossone G (7): an amorphous solid; $[\alpha]^{25}_D$ +18 (*c* 0.1, MeOH); UV (MeOH) λ_{max} (log ε) 210 (3.65), 290 (3.01) nm; ECD (*c* 1.3 × 10^{-4} M, MeOH) λ_{max} ($\Delta\varepsilon$) 213 (+18.18), 297 (−10.10) nm; IR (KBr) ν_{max} 2925, 2872, 1735, 1710, 1456, 1377, 1237, 1017, 974, 880 cm^{-1}; ^{1}H NMR see Table 1 and ^{13}C NMR see Table 2; HRESIMS m/z

378.2644 [M + NH$_4$]$^+$ (calcd for C$_{22}$H$_{36}$O$_4$N, 378.2639).

Jatrogossone H (8): colorless crystals; mp 183−185 °C; [α]$^{25}_D$ +62 (*c* 0.1, MeOH); UV (MeOH) λ_{max} (log ε) 210 (3.36) nm; ECD (*c* 1.2 × 10$^{−4}$ M, MeOH) λ_{max} ($\Delta\varepsilon$) 250 (+1.16), 323 (+0.48) nm; IR (KBr) ν_{max} 2956, 1751, 1697, 1378, 1062 cm$^{−1}$; ^{1}H NMR see Table 1 and ^{13}C NMR see Table 2; HRESIMS *m/z* 337.1799 [M + Na]$^+$ (calcd for C$_{20}$H$_{26}$O$_3$Na, 337.1774).

Jatrogossone I (9): white powder; [α]$^{25}_D$ −40 (*c* 0.1, MeOH); UV (MeOH) λ_{max} (log ε) 208 (3.45) nm; ECD (*c* 1.2 × 10$^{−4}$ M, MeOH) λ_{max} ($\Delta\varepsilon$) 250 (+1.07), 323 (+0.51) nm; IR (KBr) ν_{max} 2957, 2926, 1748, 1698, 1456, 1377, 1237, 1086, 1017, 891, 725 cm$^{−1}$; ^{1}H NMR see Table 1 and ^{13}C NMR see Table 2; HRESIMS *m/z* 337.1764 [M + Na]$^+$ (calcd for C$_{20}$H$_{26}$O$_3$Na, 337.1774).

Integerrimene (10): colorless crystals; mp 171−173 °C; [α]$^{25}_D$ −21 (*c* 0.2, MeOH); UV (MeOH) λ_{max} (log ε) 208 (3.58) nm; ECD (*c* 1.2 × 10$^{−4}$ M, MeOH) λ_{max} ($\Delta\varepsilon$) 200 (+4.66), 315 (−2.50) nm; IR (KBr) ν_{max} 2962 2931, 1733, 1714, 1455, 1370, 1238, 1016, 986, 896 cm$^{−1}$; HRESIMS *m/z* 376.2487 [M + NH$_4$]$^+$ (calcd for C$_{22}$H$_{34}$O$_4$N, 376.2482).

Cell Culture. RKO and LOVO human colon cancer cell lines were obtained from Cell Bank of Chinese Academy of Sciences (Shanghai, China). Cells were cultivated in MEM or RPMI supplemented with 10% fetal bovine serum and 1% penicillin and streptomycin at 37 °C in a humidified incubator containing 5% CO$_2$.

Cell Viability Assay. Cell proliferation was analyzed using WST-8 Cell Counting Kit-8. RKO cells were suspended in fresh MEM at a density of 6−8 × 10^4 cells/mL in a 96-well plate. Cells were treated with jatrogrossidione at various concentrations (0.625,

1.25, 2.5, 5, 10, 20, and 40 μM) for 48 h, and CCK-8 solution (10 μL) was added to the cultures and incubated for 1 h at 37 °C. A microplate reader (American Bio-Tek) at 450 nm was used to measure the optical density. The percentage of survivors in untreated control wells represented the survival of the cells. Assays were conducted as three independent experiments.

DAPI Staining. After a 24 h treatment with jatrogrossidione at the IC_{50} and 2-fold IC_{50} concentrations, DMSO, and 5-FU, cells were settled in 4% paraformaldehyde for 10 min and washed three times with phosphate-buffered saline (PBS). The cells were incubated with DAPI (Beyotime, Jiangsu, China) for 15 min, and washed again three times with PBS. Finally, the DAPI-stained cells were photographed using a fluorescence microscope (Olympus IX-73, Tokyo, Japan).

Cell Migration Assay. The RKO cells were seeded in six-well dishes and reached over 90% confluence in the wells. The cell monolayer was wounded by a sterile 100 μL tip, and the debris was washed with PBS. Afterwards, the RKO cells were transferred to 2% fetal bovine serum MEM medium at 37 °C. The cells were added sequentially: DMSO, 5-FU, or jatrogrossidione at 1/2-fold IC_{50} and IC_{50} concentrations. The migration of cells into wounded areas was measured and photographed at 0 h and 48 h with an inverted microscope. The areas of the scratches were analyzed by Image-Pro Plus 6.0 software.

Cell Cycle Analysis. The RKO cells were processed with DMSO, 5-FU or jatrogrossidione at IC_{50} and 2-fold IC_{50} concentrations at 37 °C for 24 h in a 6-well plate, harvested, and washed twice with PBS. A volume containing 1×10^6 cells were

settled with 1 mL ice-cold 70% (v/v) EtOH, and deposited at 4 °C, and finally stained with PI solution containing RNase at 37 °C for 30 min. The cell cycle was assayed by a FACSCalibur flow cytometer (BD Biosciences) and the proportion of cells at various periods was calculated by the Modfit LT 5.0 software.

Flow Cytometric Analysis of Cell Apoptosis. The intensity of apoptosis of cells was evaluated through the annexin V-fluorescein isothiocyanate (FITC) apoptosis detection kit, according to the manufacturer's instructions. The RKO cells were incubated with DMSO, 5-FU, or jatrogrossidione at IC_{50} and 2-fold IC_{50} concentrations at 37 °C in a six-well plate for 24 h, collected and washed twice with PBS, gently resuspended in binding buffer, incubated with annexin V-FITC (5 μL) and PI (5 μL) in the dark for 20 min at 37 °C, and analyzed immediately by flow cytometry.

ASSOCIATED CONTENT

Supporting Information

The Supporting Information is available free of charge on the ACS Publications Website.

IR, HRESIMS, 1D and 2D NMR spectra of **1−10**, 1D NMR spectra of **11−15**, and CD spectra of **1−10** (PDF).

Crystallographic information files for compounds **1**, **8**, and **10** (CIF).

AUTHOR INFORMATION

Corresponding Author

*Tel: +86-21-58670561-6449, E-mail: jyzhu@foxmail.com (J.-Y. Zhu).

*Tel: +86-21-58670561-6388, E-mail: hqzhang51@126.com (H. Zhang).

ORCID

Jian-Yong Zhu: 0000-0001-5922-9326

Notes

The authors declare no competing financial interest.

REFERENCES

(1) Torre, L. A.; Bray, F.; Siegel, R. L.; Ferlay, J.; Lortet-Tieulent, J.; Jemal, A. *CA Cancer J. Clin.* **2015**, *65*, 87-108.

(2) Hwang, I. H.; Oh, J.; Zhou, W.; Park, S.; Kim, J. H.; Chittiboyina, A. G.; Ferreira, D.; Song, G. Y.; Oh, S.; Na, M.; Hamann, M. T. *J. Nat. Prod.* **2015**, *78*, 453-461.

(3) Janne, P. A.; Mayer, R. J. *N. Engl. J. Med.* **2000**, *342*, 1960−1968.

(4) Ye, Y.; Xiao, L.; Wang, S. J.; Yue, W.; Yin, Q. S.; Sun, M. Y.; Xia, W.; Shao, Z. Y.; Zhang, H. *Oncotarget* **2016**, *7*, 3921-3933.

(5) Félix-Silva, J.; Giordani, R. B.; Da, S. J. A.; Zucolotto, S. M.; Fernandes-Pedrosa, M. F. *Evid-based Compl. Alt. Med.* **2014**, *12*, 982-986.

(6) Sabandar, C. W.; Ahmat, N.; Jaafar, F. M.; Sahidin, I. *Phytochemistry* **2013**, *85*, 7-

29.

(7) Ravindranath, N.; Venkataiah, B.; Ramesh, C.; Jayaprakash, P.; Das, B. *Chem. Pharm. Bull.* **2003**, *51*, 870-871.

(8) Kozhiparambil, K.; Purushothaman; Sundaram, C.; Cameron, A. F.; Connolly, J. D.; Labbé, C.; Maltz, A.; Rycroft, D. S. *Tetrahedron Lett.* **1979**, *20*, 979-980.

(9) Kupchan, S. M.; Sigel, C. W.; Matz, M. J.; Gilmore, C. J.; Bryan, R. F. *J. Am. Chem. Soc.* **1976**, *98*, 2295-2300.

(10) Kupchan, S. M.; Sigel, C. W.; Matz, M. J.; Saenz, R. J. A.; Haltiwanger, R. C.; Bryan, R. F. *J. Amer. Chem. Soc.* **1970**, *92*, 4476-4477.

(11) Das, B.; Das, R. *Phytochemistry* **1995**, *40*, 931-932.

(12) Das, R.; Das, B.; Kashinatham, A. *Nat. Prod. Sci.* **1998**, *4*, 238-240.

(13) Zhang, X. P.; Zhang, M. L.; Su, X. H.; Huo, C. H.; Gu, Y. C.; Shi, Q. W. *Chem Biodivers.* **2009**, *6*, 2166-2183.

(14) Tinto, W. F.; John, L. M. D.; Reynolds, W. F.; McLean, S. *J. Nat. Prod.* **1992**, *55*, 807-809.

(15) Zhu, J. Y.; Wang, R. M.; Lou, L. L.; Li, W.; Tang, G. H.; Bu, X. Z.; Yin, S. *J. Med. Chem.* **2016**, *59*, 6353-6369.

(16) Zhu, J. Y.; Lou, L. L.; Guo, Y. Q.; Li, W.; Guo, Y. H.; Bao, J. M.; Tang, G. H.; Bu, X. Z.; Yin, S. *RSC Adv.* **2015**, *46*, 47235-47243.

(17) Sutthivaiyakit, S.; Mongkolvisut, W.; Ponsitipiboon, P.; Prabpai, S.; Kongsaeree, P.; Ruchirawat, S.; Mahidol, C. *Tetrahedron Lett.* **2003**, *44*, 3637-3640.

(18) Bao, J. M.; Su, Z. Y.; Lou, L. L.; Zhu, J. Y.; Tang, G. H.; Gan, L. S.; Bu, X. Z.; Yin, S. *RSC Adv.* **2015**, *5*, 62921-62925.

(19) Torrance, S. J.; Wiedhopf, R. M.; Cole, J. R.; Arora, S. K.; Bates, R. B.; Beavers, W. A.; Cutler, R. S. *J. Org. Chem.* **1976**, *41*, 1855-1857.

(20) Jakupovic, J.; Grenz, M.; Schmeda-Hirschmann, G. *Phytochemistry* **1988**, *27*, 2997-2998.

(21) Villarreal, A. M.; Dominguez, X. A.; Williams, H. J.; Scott, A. I.; Reibenspies, J. *J. Nat. Prod.* **1988**, *51*, 749-753.

(22) Quan, K. T.; Park, H. S.; Oh, J.; Park, H. B.; Ferreira, D.; Myung, C. S.; Na, M. K.

Table 1. ^{1}H NMR Data of Jatrogossones A−G (1−9) in CDCl$_3$ (600 MHz, δ in ppm, J in Hz)
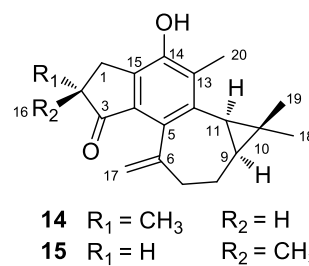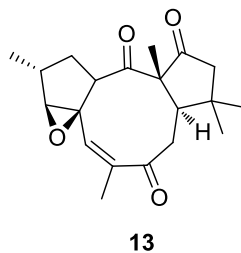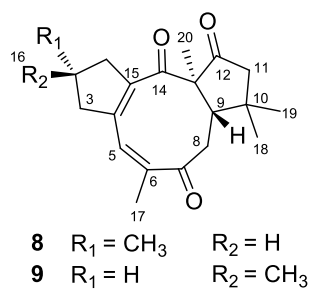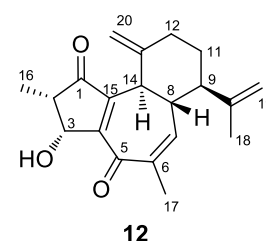
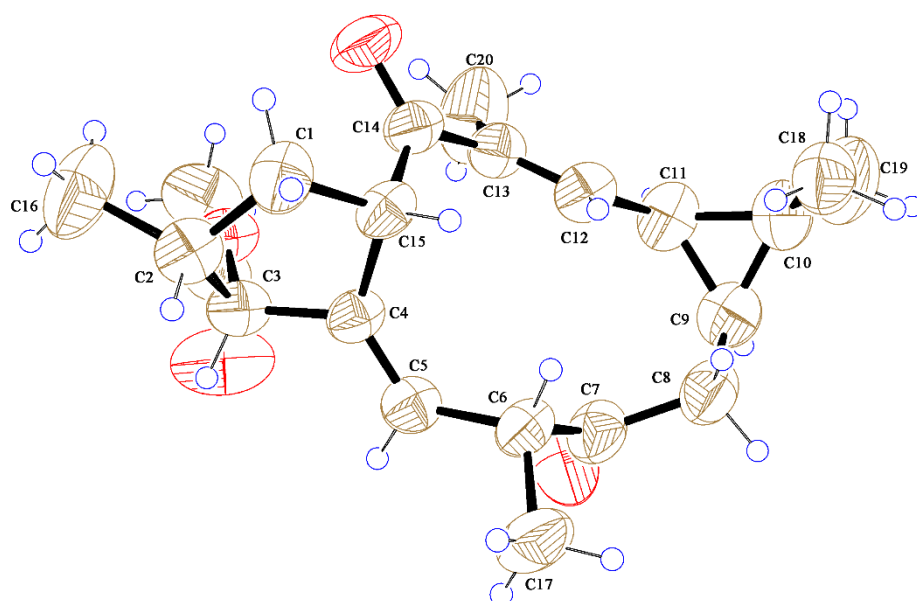| position	1	2	3	4	5	6	7	8	9
1a	2.17, m	2.04, m	2.20, dd (15.0, 8.3)	2.15, dt (12.5, 8.7)	2.19, dd (13.0, 9.0)	1.89, m	2.04, m	2.70, m	2.71, m
1b	2.04, m	1.72, m	1.99, m	1.80, ddd (12.5, 10.8, 7.5)	1.48, m	1.83, m	1.91, m	2.19, m	2.15, m
2	2.06, m	2.61, m	2.02, m	2.03, m	1.88, m	2.13, m	1.90, m	2.41, m	2.46, m
3	5.41, d (4.9)	5.80, d (5.2)	5.10, d (3.9)	5.27, d (4.6)	4.00, dd (10.2, 4.0)	5.26, dd (5.6, 5.4); 3.72, m	5.40, d (3.6)	2.59, m; 2.06, m	2.56, m; 2.06, m
4						3.72, m			
5	5.86, dd (10.4, 2.1)	6.07, d (11.0)	5.77, dd (10.3, 1.9)	6.06, d (1.8)	5.57, d (10.0)	5.36, dd (10.7, 1.4)	5.80, dd (3.3, 3.2)	5.82, s	5.81, d (1.6)
6	3.31, dd (10.4,7.1)	2.98, dd (11.0,7.0)	3.68, dd (10.3, 6.6)		3.30, m		3.43, m		
8a	2.52, dd (14.8, 7.1)	2.40, dd (14.6, 5.7)	2.46, dd (13.4, 1.4)	3.41, dd (11.9, 11.8)	2.76, dd (11.5, 11.4)	2.92, dd (15.3, 5.9)	2.22, d (9.6)	2.80, dd (14.2, 2.9)	2.77, dd (14.2, 2.9)

8b	2.28, dd (14.8, 10.9)	2.09, m	2.10, dd (13.4, 10.8)	2.36, dd (11.9, 3.9)	2.40, dd (11.0, 3.9)	2.49, dd (15.3, 12.2)		2.51, d (14.2)	2.50, d (14.2)
9	1.62, m	1.70, m	0.59, m	2.98, m	2.91, m	3.10, m	1.34, dd (9.6, 9.3)	2.61, d (2.9)	2.62, d (2.9)
11a	1.39, dd (9.7, 9.6)	1.42, dd (9.7, 9.6)	0.36, m'	5.60, dd (15.4, 9.7)	5.67, dd (15.2, 10.1)	5.44, dd (15.0, 10.1)	0.83, m	2.55, d (16.3)	2.56, d (16.3)
11b								2.31, d (16.3)	2.30, d (16.3)
12a	5.78, dd (9.7, 1.3)	6.26, d (9.8)	1.94, m	5.23, dd (15.4, 9.2)	5.00, dd (15.2, 9.9)	4.92, dd (15.0, 10.1)	1.54, m		
12b			1.22, m				1.06, m		
13			3.21, m	3.24, dd (9.2, 6.9)	3.45, dd (9.9, 6.5)		2.17, dd (13.9, 6.7)		
15	3.71, dd (8.0, 2.2)		3.78, m	4.12, dd (8.5, 8.2)	1.77, m	3.22, m	2.96, m		
16	1.00, d (6.4)	1.01, d (6.9)	1.04, d (6.2)	1.02, d (6.8)	1.09, d (6.7)	0.95, d (6.9)	0.97, d (6.2)	1.07, d (6.9)	1.03, d (6.8)
17	1.16, d (7.1)	1.11, d (7.0)	1.16, d (6.7)	1.37, s	1.21, d (7.2)	1.93, d (1.43)	1.23, d (6.9)	1.91, d (1.6)	1.91, d (1.6)
18	1.13, s	1.25, s	0.82, s	1.75, s	1.75, s	1.73, s	0.94, s	0.88 , s	0.88 , s
19a	1.19, s	1.15, s	0.96, s	4.81, s	4.84, s	4.79, s	1.06, s	1.28, s	1.27, s
19b				4.79, s	4.77, s	4.76, s			
20	1.77, d (1.3)	1.88, s	1.11, d (6.7)	1.24, d (6.9)	1.13, d (6.5)	1.09, d (6.5)	1.13, d (7.3)	1.36, s	1.34, s
3-OAc	2.01, s	2.10, s	1.96, s	2.10, s		2.11, s	2.01, s		

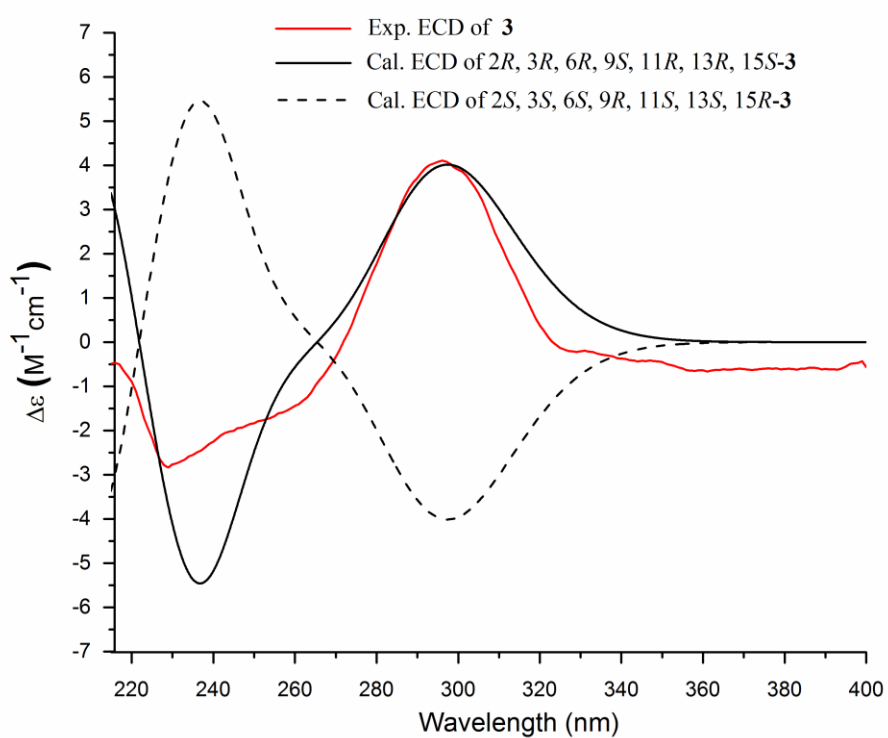**Table 2. ^{13}C NMR Data of Jatrogossones A−G (1−9) in CDCl$_3$ (150 MHz, δ in ppm)**

position	1	2	3	4	5	6	7	8	9
1	33.6, CH$_2$	47.3, CH$_2$	33.0, CH$_2$	36.8, CH$_2$	37.2, CH$_2$	35.5, CH$_2$	33.8, CH$_2$	44.9, CH$_2$	44.8, CH$_2$
2	37.2, CH	36.1, CH	37.4, CH	36.8, CH	39.8, CH	37.5, CH	37.2, CH	32.8, CH	32.5, CH
3	80.5, CH	79.3, CH	81.8, CH	82.7, CH	79.9, CH	78.5, CH	80.4, CH	45.1, CH$_2$	45.2, CH$_2$
4	139.9, C	138.6, C	139.4, C	140.2, C	143.1, C	44.6, CH	144.9, C	141.9, C	141.8, C
5	131.3, CH	135.8, CH	132.1, CH	134.8, CH	127.0, CH	132.2, CH	132.1, CH	127.6, C	127.8, C
6	50.2, CH	50.2, CH	47.9, CH	80.3, C	49.0, CH	139.1, C	47.7, CH	141.6, C	141.4, C
7	213.6, C	213.2, C	210.9, C	212.4, C	211.1, C	205.7, C	207.3, C	208.8, C	208.9, C
8	36.7, CH$_2$	36.8, CH$_2$	39.5, CH$_2$	41.3, CH$_2$	45.0, CH$_2$	47.1, CH$_2$	59.2, CH	39.3, CH$_2$	39.2, CH$_2$
9	30.5, CH	32.6, CH	23.5, CH	47.7, CH	48.8, CH	46.6, CH	20.0, CH	51.4, CH	51.3, CH
10	23.2, C	24.2, C	18.4, C	146.2, C	145.6, C	145.9, C	17.6, C	37.4, C	37.4, C
11	25.9, CH	26.0, CH	23.4, CH	134.4, CH	134.8, CH	132.7, CH	18.3, CH	55.8, CH$_2$	55.8, CH$_2$
12	134.3, CH	143.7, CH	28.4, CH$_2$	131.5, CH	131.0, CH	132.3, CH	26.5, CH$_2$	215.3, C	215.4, C
13	142.0, C	138.6, C	43.9, CH	53.1, CH	53.0, CH	52.5, CH	38.5, CH	64.6, C	64.3, C

14	204.0, C	205.7, C	210.5, C	208.6, C	216.0, C	210.2, C	78.6, C	213.3, C	213.0, C
15	51.7, CH	83.3, C	52.6, CH	51.0, C	50.6, C	53.0, CH	54.6, CH	138.3, C	138.1, C
16	13.9, CH$_3$	13.0, CH$_3$	13.6, CH$_3$	13.7, CH$_3$	13.6, CH$_3$	14.8, CH$_3$	13.4, CH$_3$	21.7, CH$_3$	20.9, CH$_3$
17	18.0, CH$_3$	17.4, CH$_3$	17.5, CH$_3$	29.2, CH$_3$	17.6, CH$_3$	20.3, CH$_3$	15.1, CH$_3$	19.3,CH$_3$	19.4,CH$_3$
18	15.6, CH$_3$	15.5, CH$_3$	15.3, CH$_3$	21.4, CH$_3$	21.3, CH$_3$	21.1, CH$_3$	14.8, CH$_3$	27.8, CH$_3$	27.9, CH$_3$
19	28.3, CH$_3$	28.2, CH$_3$	28.5, CH$_3$	110.4, CH$_2$	110.2, CH$_2$	110.7, CH$_2$	28.3, CH$_3$	23.8, CH$_3$	23.8, CH$_3$
20	14.2, CH$_3$	13.7, CH$_3$	18.2, CH$_3$	16.6, CH$_3$	16.0, CH$_3$	15.7, CH$_3$	18.3, CH$_3$	14.9, CH$_3$	14.8, CH$_3$
3-OAc	170.3, C	170.5, C	170.9	170.9		170.9	170.6		
	21.2, CH$_3$	21.3, CH$_3$	21.3, CH$_3$	21.3, CH$_3$		21.0, CH$_3$	21.4, CH$_3$		

1 R$_1$ = H
2 R$_1$ = OH

3

4 R$_1$ = OAc R$_2$ = OH
5 R$_1$ = OH R$_2$ = H
10 R$_1$ = OAc R$_2$ = H

6

7

11

12

8 R$_1$ = CH$_3$ R$_2$ = H
9 R$_1$ = H R$_2$ = CH$_3$

13

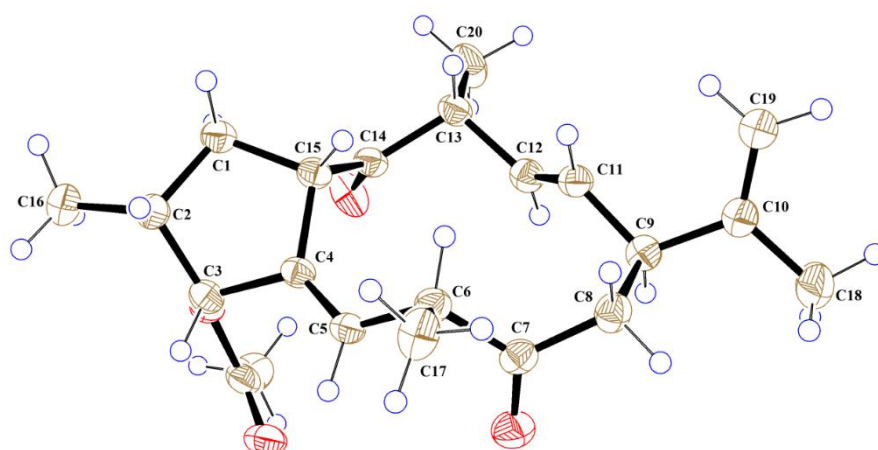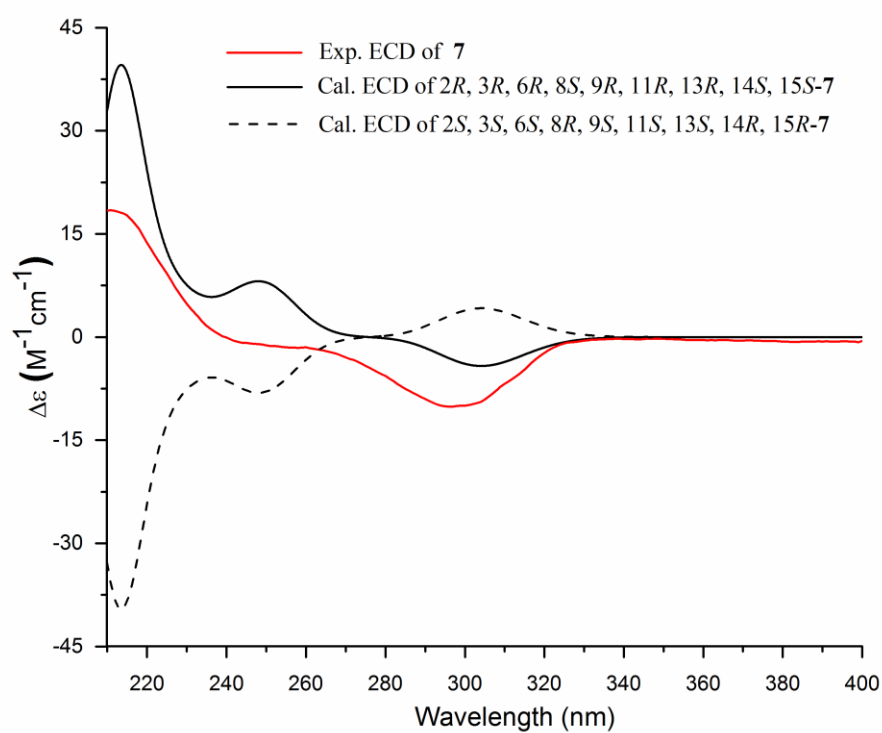**14** R$_1$ = CH$_3$ R$_2$ = H
15 R$_1$ = H R$_2$ = CH$_3$
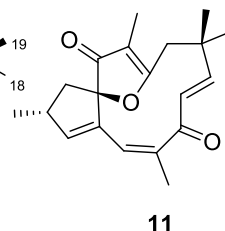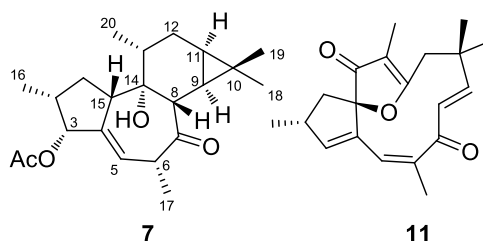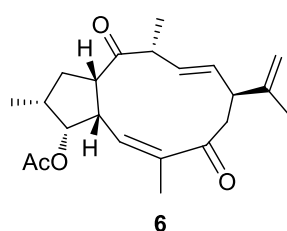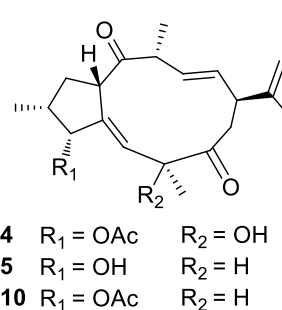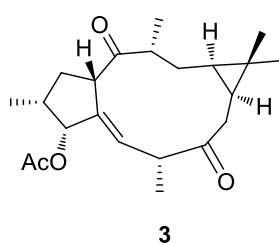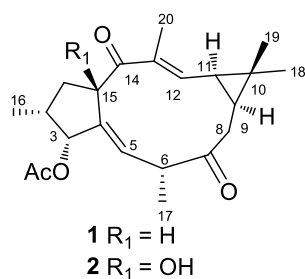
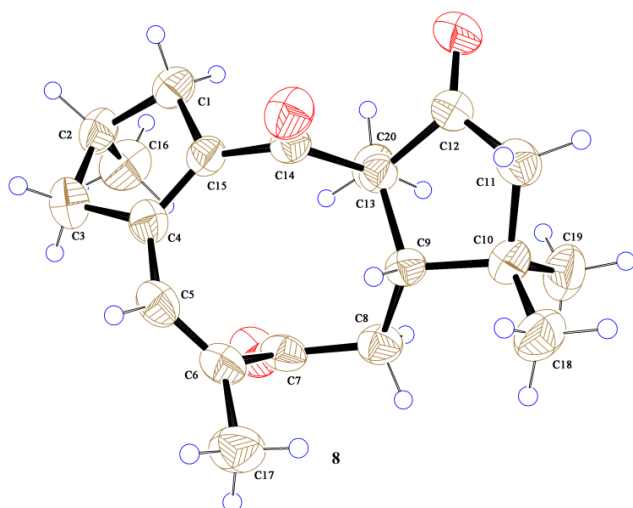**Figure 1.** ORTEP diagram of compound **1**.

Figure 2. Experimental ECD spectrum (210–400 nm) of **3** and the calculated ECD spectra of the model molecules of **3** at the B3LYP/6-311++G (d, p) level in the gas phase.
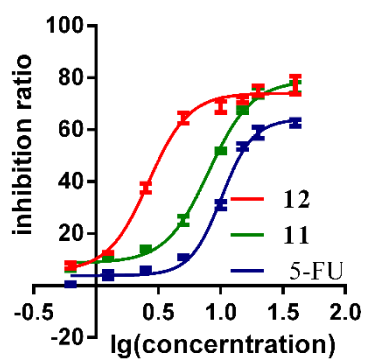
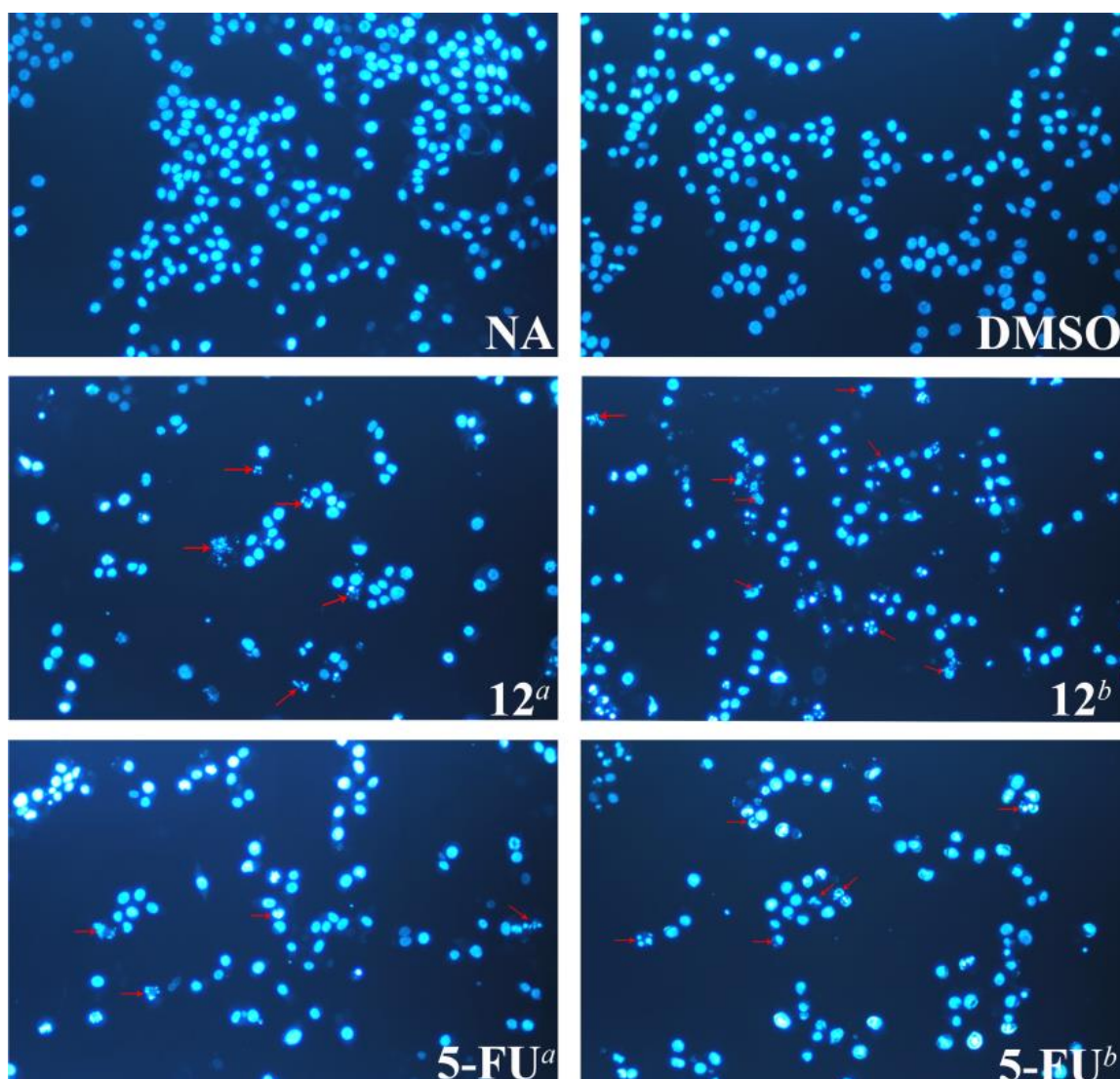**Figure 3.** ORTEP diagram of compound **10**.

Figure 4. Experimental ECD spectrum (210–400 nm) of **7** and the calculated ECD spectra of the model molecules of **7** at the B3LYP/6-311++G(d, p) level in the gas phase.

**Figure 5.** ORTEP diagram of compound **8**.

Figure 6. Inhibitory curves of compounds **11**, **12**, and 5-FU (positive control) in RKO cells.

Figure 7. Evaluation of effects on apoptosis by compound **12**. Evaluation of changes in nuclear morphology by fluorescence microscopy of DAPI-stained nuclei after 24 h of incubation of RKO human colon cancer cells with compounds **12**, 5-FU, or DMSO vehicle control. Representative images of compound effect on apoptosis (200 × magnification), with red arrows highlighting apoptotic cells. [a]IC_{50}, [b]2-fold IC_{50}.
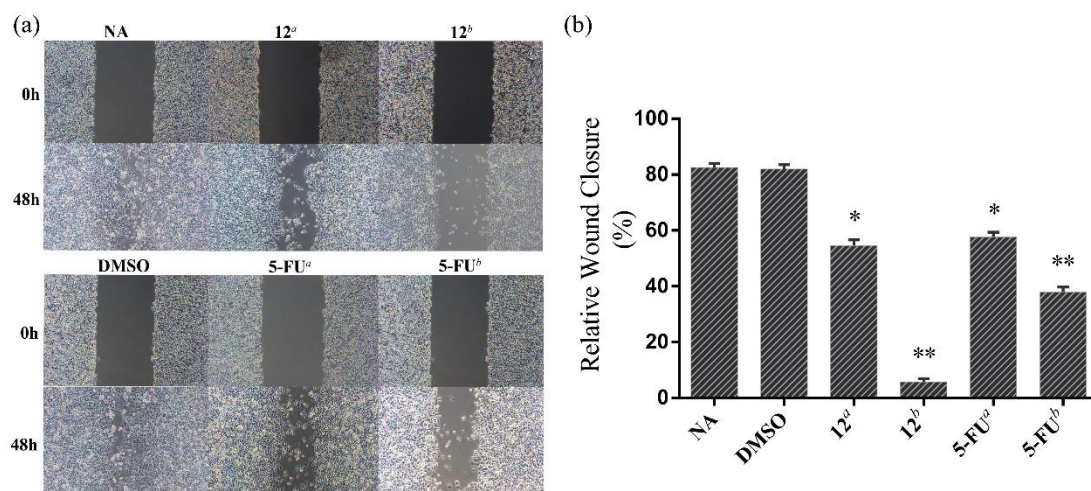
Figure 8. Wound-healing assays by compound **12** with human colon cancer cell RKO. The incubation of **12**, 5-FU, or DMSO with tumor cells (a). The antimigration effects of **12**, 5-FU, or DMSO on the tumor cells (b). ^{a}1/2-fold IC$_{50}$, ^{b}IC$_{50}$, $^*p < 0.05$, $^{**}p < 0.01$.
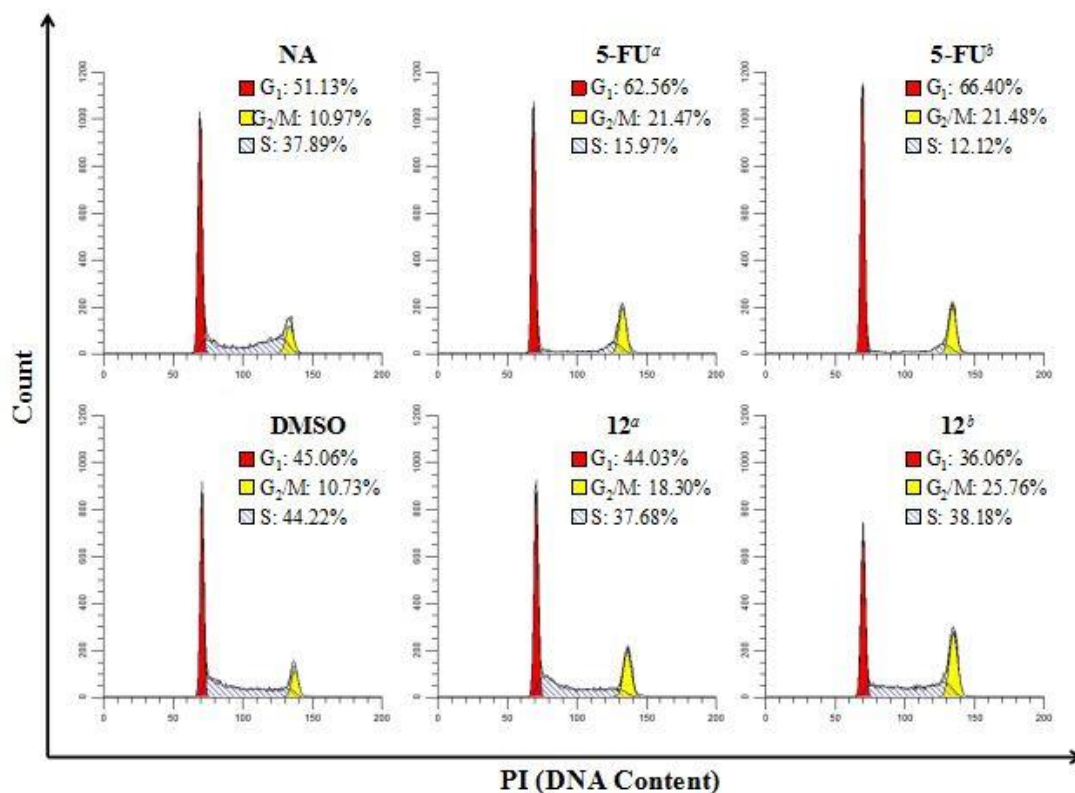
Figure 9. Effects of compound **12** on cell cycle distribution. RKO human colon cancer cells were treated with compounds **12**, 5-FU, or DMSO vehicle control for 24 h then harvested, stained with PI, and analyzed by flow cytometry. Following flow cytometry analysis, frequencies of cells in each phase of the cell cycle were calculated using Mod Fit LT 5.1 software. ^{a}IC$_{50}$, ^{b}2-fold IC$_{50}$.
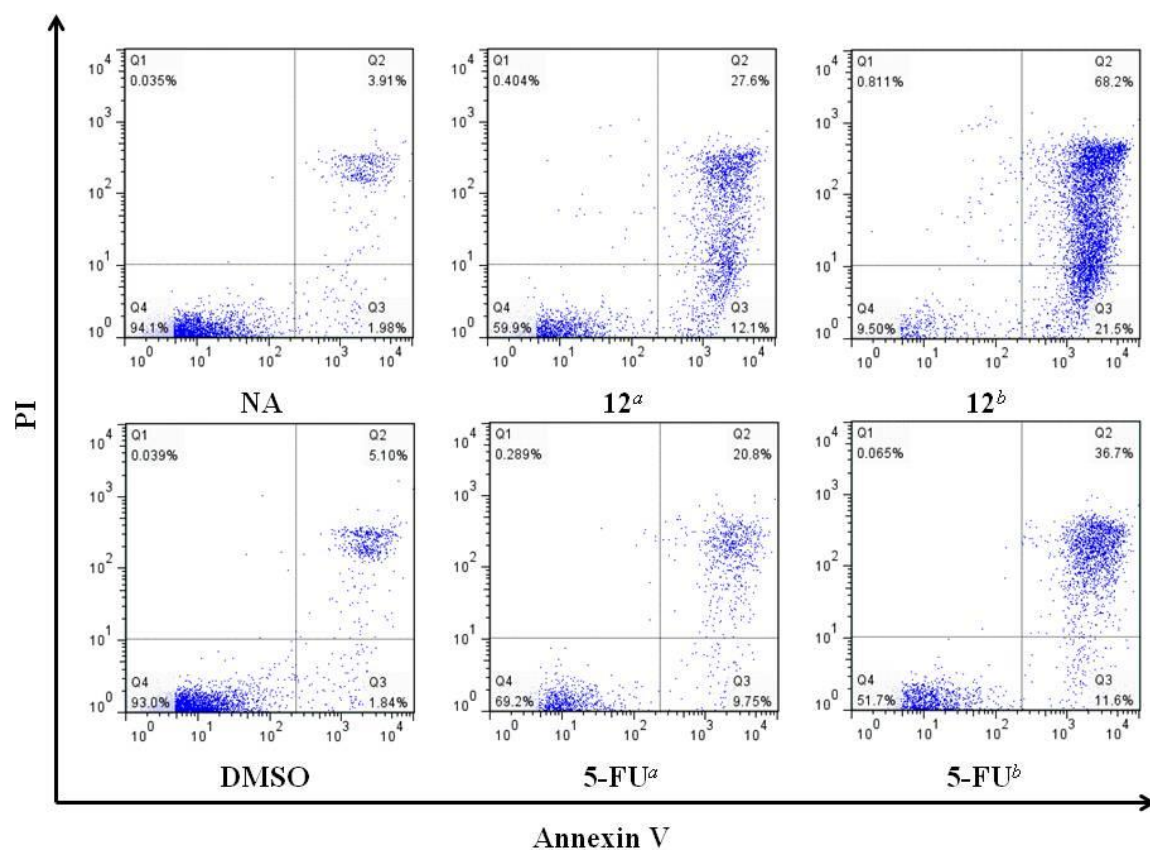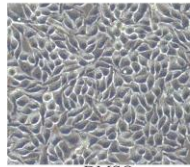
Figure 10. Apoptosis in RKO cells induced by **12**. RKO cells were treated with **12**, 5-FU, or DMSO for 24 h and then harvested, stained with annexin V/PI, and analyzed by flow cytometry. [a]IC_{50}, [b]2-fold IC_{50}.
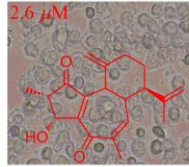
TOC:

Jatropha gossypiifolia DMSO **12**